CROSSBAR H-MODE DRIFT-TUBE LINAC DESIGN WITH ALTERNATIVE PHASE FOCUSING FOR MUON LINAC

M. Otani, K. Futatsukawa, KEK, Oho, Tsukuba, 305-0801, Japan
K. Hasegawa, Y. Kondo, JAEA, Tokai, Naka, Ibaraki, 319-1195, Japan
R. Kitamura, University of Tokyo, Hongo, 113-8654, Japan
S. Kurennoy, Los Alamos, NM, 87545, USA

Abstract

We have developed a Crossbar H-mode (CH) drift-tube linac (DTL) design with an alternative phase focusing (APF) scheme for a muon linac, in order to measure the anomalous magnetic moment and electric dipole moment (EDM) of muons at the Japan Proton Accelerator Research Complex (J-PARC). The CH-DTL accelerates muons from $\beta = v/c =$ 0.08 to 0.28 at an operational frequency of 324 MHz. The design and results are described in this paper.

INTRODUCTION

The use of a low emittance muon beam has been discussed in several scientific fields [1–4]. One of those is the quest for hunting beyond the Standard Model (SM) of elementary particle physics. In the muon anomalous magnetic moment $(g-2)_\mu$, the SM prediction and the measured value with a precision of 0.54 ppm [5] differs by about three standard deviations. Since this is considered to be due to unknown interactions or particles in the SM, further investigations are desirable. The low emittance muon beam will provide more precise measurements since the dominant systematic uncertainties in the previous experiment [5] resulted from the muon beam dynamics in the muon storage ring.

We are developing a muon linac for the $(g-2)_\mu$ experiment [6] at the Japan Proton Accelerator Research Complex (J-PARC) to produce the low emittance muon beam. Details of the muon linac configuration can be found in [7]. Although conventional linacs adopt Alvarez DTLs after radio-frequency quadrupoles, an H-mode DTL is employed during the particle velocity β =0.08 to 0.28 (4.5 MeV) stage, so as to yield a higher acceleration efficiency. In order to achieve more efficient acceleration, the alternating phase focusing (APF) method is adopted.

There are two candidates for the room-temperature H-mode structure. One is an inter-digital H-mode (IH) structure that works in the TE_{11}-mode, while the other is a Crossbar H-mode (CH) operated in the TE_{21}-mode [8]. Our first effort has been devoted to the IH structure. Though our design [9] satisfies the experimental requirement, there is a substantial emittance growth in the vertical direction, generated from the dipole component of the RF electric field. The dipole field is an unavoidable issue in an IH structure and can potentially deteriorate the beam quality. On the other hand, there is no dipole field in a CH structure and better quality of the output beam is expected. However, the CH structure has never been designed and used with the APF method.

Following sections in this paper describe the design procedures and results of the APF CH-DTL for the muon linac.

SYNCHRONOUS PHASE ARRAY OPTIMIZATION

In this step, the particle dynamics are calculated analytically using certain approximations and for a particular synchronous phase array. These calculations are performed using "LINACSapf" [10], with some modifications for the dynamics calculations and the synchronized phase array definition to accommodate the π–mode acceleration, whereas 2π–mode acceleration is assumed in the original code. Details of the approximation method can be found in [9, 10].

Table 1 shows the optimized phase array results. Gap numbers 1–2, 6–9, 15 and 16 have negative synchronous phases, during which time the beam is longitudinally focused. However, gap numbers 3–5 and 10–14 have positive phases, during which the beam is transversely focused. Because the electrostatic focusing effect is stronger in the lower-β part, the first collection of positive phase groups has a smaller number of gaps. The output energy is 4.5 MeV and the total length is 1.3 m.

Table 1: Cell Parameters for Optimized Phase Array

Cell	W [MeV]	β	ϕ [degrees]	Cell length [mm]	Total length [mm]
1	0.34	0.08	-35.9	29.5	29.5
2	0.43	0.09	-14.9	46.0	75.4
3	0.57	0.10	12.9	54.9	130
4	0.74	0.12	32.9	60.3	191
5	0.92	0.13	15.4	54.4	245
6	1.14	0.15	-13.8	56.0	301
7	1.38	0.16	-31.4	66.4	367
8	1.63	0.17	-44.3	74.1	442
9	1.86	0.19	-18.8	97.2	539
10	2.16	0.20	12.5	108	646
11	2.49	0.21	27.6	106	753
12	2.82	0.23	47.6	116	868
13	3.10	0.24	23.2	94.2	963
14	3.50	0.25	10.8	108	1070
15	3.95	0.27	-34.6	91.5	1160
16	4.30	0.28	-15.6	142	1300
exit	4.50				

Figure 1 shows the expected output beam with the analytical calculation. Here the input beam is a water-bag distribution with the expected twiss parameters. The emittance growth during the acceleration is expected to be a few percent, which satisfies our requirement.

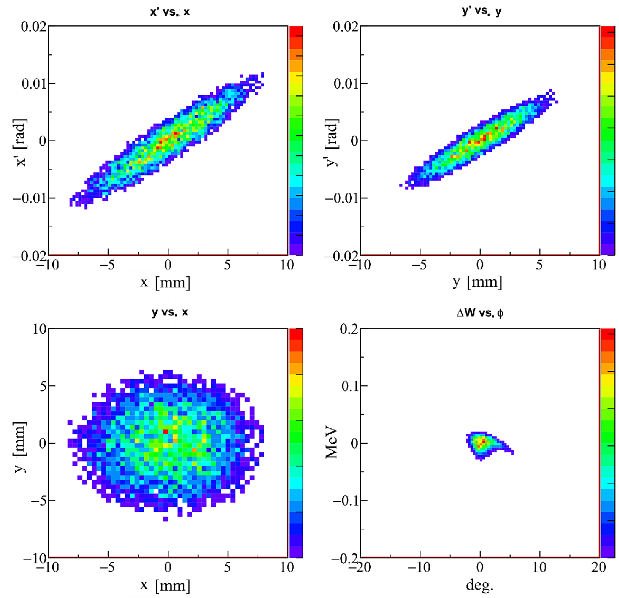

Figure 1: Expected output beam distributions based on the analytical beam dynamics calculation.

CH CAVITY OPTIMIZATION

Because a CH cavity is not axially symmetric, a three-dimensional model is necessary in order to evaluate the electro-magnetic field. In addition, the electro-magnetic field and the resonant frequency depend on the structure of the cavity, and detailed information of the overall structure (including ridges, etc.) should thus be incorporated in the calculation model. Therefore, the entire CH cavity is modeled using the CST Micro Wave (MW) Studio [11] three-dimensional field solver, in order to calculate the electro-magnetic field. Figure 2 shows the three-dimensional model of the CH cavity in CST MW Studio. The CH cavity consists of a cylindrical cavity and four ridges mounted on the top, bottom, left and right of the cavity. To operate the CH cavity as an accelerator in the TE_{21}-mode, drift tubes are mounted alternately on the top-bottom ridges and the left-right ridges via stem pairs. The stem pairs are connected to the drift tubes at the tube centers, and front and end ridge-cuts are present in all the ridges (ridge tuners). The inner radius of the cavity is tapered in the down- to upstream direction (cavity taper). The ridge tuner shape and the cavity taper are varied in order to adjust the flatness of the electric field. In the IH case, the cavity is designed in the same manner as the CH case except mounting of the drift tubes; the drift tubes are mounted alternately on the top and bottom ridges via stems and there are no left and right ridges [9].

The drift tubes and the acceleration gaps are first arranged according to the previously determined optimized parameters shown in Table 2. To optimize the acceleration field, other dimensions are optimized. Especially the length of the back ridge tuner is changed to modify the non-uniformity of the field in upstream and downstream directions. Then, small differences in the field between the gaps due to the gap length difference is adjusted by changing the drift tube outer radius.

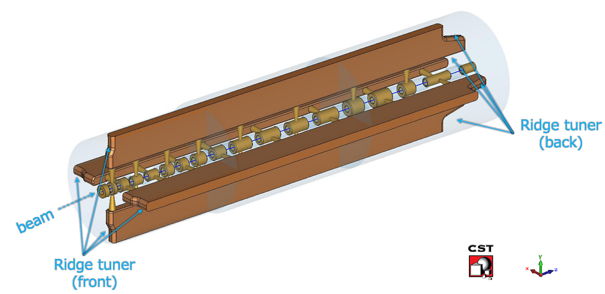

Figure 2: Three-dimensional model of the CH cavity in CST MW Studio calculation.

Figure 3 shows the longitudinal (red) and vertical (green) electric field along the beam axis after these optimizations. The variation in the longitudinal electric field in the gaps is approximately 15%, excluding the first and last cells. Further optimization for the first and last cells will be attained by changing the gap lengths. The vertical field is less than 1% of the longitudinal field, whereas it is about 10% in the IH case.

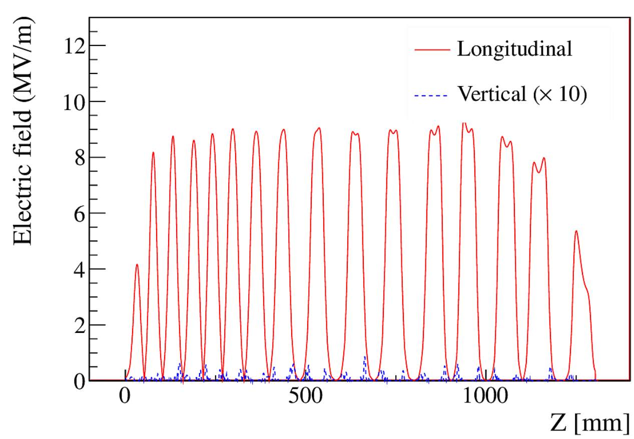

Figure 3: Longitudinal (solid red) and vertical (dotted blue) component of the electric field.

Table 2 summarizes the basic parameters of the CH cavity. Because the acceleration field is slightly reduced in the first and last cells compared to that in the analytical design, the output beam energy is smaller then that in Table 1. The maximum surface field is calculated to be 2.1 times the Kilpatrick limit. This value is slightly higher and further reduction of the maximum field will be attained through optimization of the chamfered structure at the edge of the drift tube.

PARTICLE TRACKING

Finally, the beam particle trajectory is simulated using the general particle tracer (GPT) [12]. The electric and magnetic

ISBN 978-3-95450-182-3

Table 2: Main Parameters of the CH Cavity

No. of gaps	16
Frequency (MHz)	323.48
Energy range (MeV)	0.3 - 4.1
Effective voltage (MV)	3.8
Q_0	14400
Power dissipation (kW)	360
Kilpatrick factor	2.1 (37.5 MV/m)

fields calculated in previous steps are incorporated in the code and the particle dynamics are calculated numerically. Figure 4 shows the normalized velocity in the y-direction along the beam axis (z). Compared to the IH case, there is no meandering due to the substantial dipole field and better output beam quality is expected.

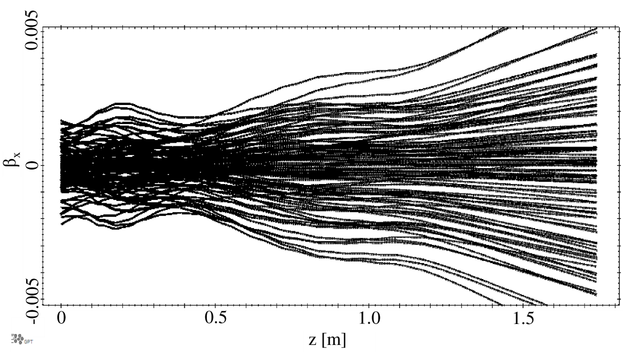

Figure 4: Normalized vertical velocity ($\beta_y = v_y/c$) along the beam axis.

Table 3 summarizes the particle simulation results. The output emittance was estimated to be 0.317π and 0.188π mm mrad in the horizontal and vertical directions, respectively. The emittance in the horizontal direction is consistent to the one obtained in the IH case within 1%. Thanks to the negligible dipole field, the emittance in the vertical direction is improved compared with the one obtained in the IH case by 4%. The transmission and survival rate are the same as those in the IH case.

Table 3: Summary of Output Beam Evaluations. IH: the output beam parameters with the IH [9]. CH: the output beam parameters with the CH

	Input	Output	
		IH	CH
β	0.08	0.28	0.27
Energy (MeV)	0.34	4.4	4.1
ε_x [π mm mrad]	0.297	0.315	0.317
ε_y [π mm mrad]	0.168	0.195	0.188
Transmission [%]		99.9	99.9
Transient time [nsec]		25	25
Survival rate [%]		98.9	98.9
Transmission total [%]		98.7	98.7

SUMMARY

In this paper, the APF CH-DTL design for the J-PARC g-2/EDM experiment has been presented. First, the synchronous phase array was optimized in order to obtain lower emittance growth, based on analytical calculations of the beam dynamics. Then, the CH cavity dimensions were optimized using finite element method calculation. Finally, the beam dynamics obtained for the calculated RF fields was evaluated via numerical calculations. Thanks to the negligible dipole field, the output beam emittance is expected to be better than the one obtained in the IH case [9].

ACKNOWLEDGMENT

The authors are grateful to R. A. Jameson for useful advice on the APF linac and on modifications of the "LINACSapf" code. This work was supported by JSPS KAKENHI Grant Numbers 15H03666, 16H03987.

REFERENCES

[1] M. Palmer et al., ICFA Beam Dynamics Newsletter, No.55, 2011, `http://icfa-usa.jlab.org/archive/newsletter/icfa_bd_nl_55.pdf`

[2] Y. Miyake et al., Hyperfine Interact, vol. 216, p.79, 2013, `https://www.researchgate.net/publication/257570151_Ultra_slow_muon_microscopy_by_laser_resonant_ionization_at_J-PARC_MUSE`

[3] M. Bogomilov et al., JINST vol. 7, p. P05009, 2012, `dx.doi.org/10.1088/1748-0221/7/05/P05009`

[4] S. Artikova et al., Proc. of PASJ'13, paper SAP045, `http://www.pasj.jp/web_publish/pasj10/proceedings/PDF/SAP0/SAP045.pdf`

[5] G.W. Bennett et al., Phys. Rev. D73, 072003, 2006, `http://journals.aps.org/prd/abstract/10.1103/PhysRevD.73.072003`

[6] J-PARC E34 conceptual design report, 2011 (unpublished), `https://kds.kek.jp/indico/event/8711/material/2/0.pdf`

[7] M. Otani et al., Proc. of IPAC'16, paper TUPMY02.

[8] S.S. Kurennoy et al., `https://journals.aps.org/prab/pdf/10.1103/PhysRevSTAB.14.110101`Phys. Rev. ST Accel. Beams 14, 110101, 2011.

[9] M. Otani et al., `https://journals.aps.org/prab/references/10.1103/PhysRevAccelBeams.19.040101`Phys. Rev. Accel. Beams, 19, 040101, 2016.

[10] R.A. Jameson, `http://arxiv.org/abs/1404.5176`arXiv:1404.5176[physics.acc-ph]

[11] CST Studio Suite, Computer Simulation Technology (CST). `https://www.cst.com/products/CSTMWS`

[12] General Particle Tracer, Pulsar Physics. `http://www.pulsar.nl/gpt/`